ANALYTICAL DISPERSION MODELS FOR EFFICIENT SIMULATION OF COMPLEX MICROCHIP ELECTROPHORESIS SYSTEMS

Y. Wang, Q. Lin, T. Mukherjee
Carnegie Mellon University, Pittsburgh, USA

ABSTRACT

This paper presents analytical band broadening models that account for skew induced dispersion for composable system simulation of electrophoretic separation microchips. The models not only accurately describe the behavior of individual components, but also capture their interactions. The validity of the models is verified by comparison to experimental data and numerical results.

Keywords: dispersion, electrophoresis, microchips, simulation

1. Introduction

While electrophoretic separation microchips have been widely studied in the past decade, their efficient design continues to be a challenge. Trial-and-error design methods involving extensive experiments and numerical computation can lead to unacceptably long design cycles. Several analytical [1, 2] and semi-analytical [3] dispersion models have been proposed to speed up microchip design. A system simulation approach in which a design is decomposed into components has been proposed [4], but involves over-simplified dispersion models that do not accurately account for component interactions. To address these issues, this paper presents closed-form, parameterized analytical dispersion models that are both accurate and efficient for composable system simulation of electrophoretic separation microchips.

2. Analytical dispersion models

Consider an electrophoretic separation column consisting of a straight channel with length L_{bt} and width w, and two complimentary turns with average radius R_c (Figure 1). An electric field E causes a charged analyte to move in a buffer solvent. The combined effects of decreasing migration distance and increasing E toward the inside wall of the turn skew and broaden the analyte band in the first turn [3]. Some of the skew may be undone in the inter-turn straight channel, leading to "overcorrection" in the second turn. This can be more pronounced in multiple turns and makes calculation of final analyte band width difficult. To address this issue, a composable simulation approach is applied (Figure 1), in which every component (turn, straight channel, *etc.*) is represented by a behavioral model and linked by appropriate interfacial parameters. Starting from the injector, each component's model sets the input values to its downstream neighbor.

Following the procedure described in [1] and assuming small value of w/R_c, we can transform the advection-diffusion equation in a turn into an unfolded Cartesian coordinate (see Eq. (1.*a*)), where c is the analyte concentration, x the longitudinal

7th International Conference on Miniaturized Chemical and Biochemical Analysis Systems
October 5–9, 2003, Squaw Valley, California USA

coordinate in the unfolded Cartesian frame, y the width-wise coordinate. The linear apparent velocity u in such Cartesian coordinate is found as $u \approx U(1+(w-2y)/R_c)$, where $U=E\mu$ is the average velocity, and μ is the analyte electrophoretic mobility. This apparent velocity accounts for both effects of migration distance and electric field variation along the channel width.

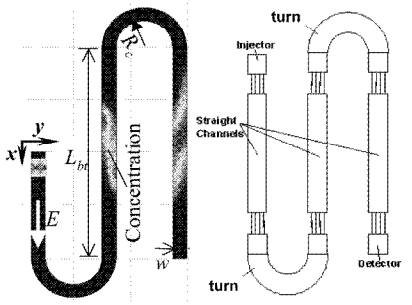

Fig. 1. Geometry and composable schematic of an electrophoresis system of two complimentary turns.

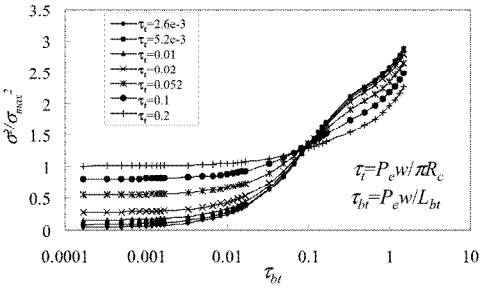

Fig. 2. The dependence of σ^2/σ_{max}^2 on τ_t and τ_{bt} in a system of two complimentary turns, where $\sigma_{max}^2=(2\pi w)^2/12$.

Adopting the method of moments [5], we can normalize the governing equation (1.*a*) in a new coordinate frame (Eq (1.*b*)) that moves at velocity U:

$$\begin{cases} \partial c/\partial t = D\cdot\nabla^2 c - u\cdot\partial c/\partial x \\ \partial c/\partial y\big|_\Gamma = 0 \\ c(x,y,0)=c_0(x,y) \end{cases} \quad (1.a) \longrightarrow \quad \begin{cases} \partial c/\partial \tau = \overline{\nabla}^2 c - P_e\cdot\chi\cdot\partial c/\partial\xi \\ \partial c/\partial \eta\big|_\Gamma = 0 \\ c(\xi,\eta,0)=c_0(\xi,\eta) \end{cases} \quad (1.b)$$

where t is the separation time, D the analyte diffusivity, $\tau=tD/w^2$ the dimensionless time indicating the ratio of transverse diffusion to axial convection in a component. Here $\xi=(x-Ut)/w$, $\eta=y/w$, $\overline{\nabla}^2=\partial^2/\partial\eta^2+\partial^2/\partial\xi^2$, Peclet number $P_e=Uw/D$, and $\chi=(u-U)/U$ the analyte velocity relative to the mean. Define $m_p(\tau)=\bar{c}_p=\int c_p d\eta$ as the p^{th} moment of the cross-section-averaged concentration of the analyte band, where $c_p(\eta,\tau)=\int_{-\infty}^{\infty}\xi^p c(\xi,\eta,\tau)d\xi$ is the p^{th} moment of the concentration in the filament through η. Then Eq. (1.*b*) can be reformulated in terms of m_p and c_p and be solved for c_1, m_0, m_1 and m_2 to provide interfacial parameters c_1 and σ^2 between components: $c_1(\eta,\tau)$ represents the location of each filament's center of gravity to characterize the band skew, $m_0(\tau)$ the total mass of the analyte band, $m_1(\tau)$ the location of the whole band's center of gravity, and σ^2 the longitudinal standard deviation (variance) of the cross-sectional average concentration. The band width (σ^2) is related to $m_2(\tau)$ through $\sigma^2=w^2(m_2/m_0-m_1^2/m_0^2)$. All of them are measured relative to a transverse plane that moves at U, a consequence of the normalization reducing Eq. (1.*a*) to Eq. (1.*b*).

Eqs. (2, 3) and Eqs. (4, 5) give the variation of c_1 and σ^2 in a turn and in a straight channel respectively based on their individual dimensionless residence time τ_t and τ_{bt}:

$$c_{1,turn}(\eta,\tau_t) = \sum_{n=odd}^{\infty} \left(\pm J_n\left(1-e^{-\lambda_n\tau_t}\right)/\lambda_n + B_n e^{-\lambda_n\tau_t}\right)\cdot\cos(n\pi\eta) \quad (2)$$

$$\Delta\sigma^2_{turn} = \left\{2\tau_t \pm \frac{8\pi}{\tau_t}\cdot\sum_{n=odd}^{\infty}\left(B_n\lambda_n\left(1-e^{-\lambda_n\tau_t}\right)\pm J_n\left(-\lambda_n\tau_t + e^{-\lambda_n\tau_t}-1\right)\right)/\lambda_n^3\right\}w^2 \quad (3)$$

$$c_{1,straight}(\eta,\tau_{bt}) = \sum_{n=odd}^{\infty} B_n e^{-\lambda_n\tau_{bt}}\cdot\cos(n\pi\eta) \quad (4)$$

$$\Delta\sigma^2_{straight} = 2w^2\tau_{bt} \quad (5)$$

where $\tau_t=\pi R_c/P_e w$, $\tau_{bt}=L_{bt}/P_e w$, $\lambda_n=(n\pi)^2$, $J_n=8P_e w/(\lambda_n R_c)$. Here B_n is the Fourier series coefficients for the input skew and $c_1(\eta, 0)=\sum B_n\cdot\cos(n\pi\eta)$. In Eq. (3), the plus sign is assigned to the first turn and any turn strengthening the skew caused by the first; the minus sign is assigned to any turn undoing the skew. The input skew's effect on the variance in the turn is considered by the first term in the summation in Eq. (3). We find that the normalized system variance σ^2/σ_{max}^2 only depends on τ_t and τ_{bt} as shown in Figure 2 for a system of two complimentary turns. At low τ_{bt} and τ_t, the final variance is low due to nearly complete skew cancellation in the two turns. At high τ_{bt}, relatively large transverse diffusion smears out the skew before the band arrives at the second turn, which overcorrects the skew. This effectively introduces another dispersion source leading to a higher final variance.

3. Simulation and verification

System simulation results from our models using mean widths of 37 μm and 50 μm [1, 3] are compared with experimental data [3] in Figures 3 and 4, showing that each subsequent turn overcorrects and increases the band dispersion due to the high τ_t and τ_{bt}.

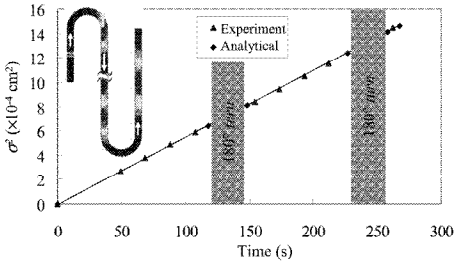

Fig. 3. Comparison of system simulation results with experimental data [3] (τ_t=3.85 and τ_{bt}=10).

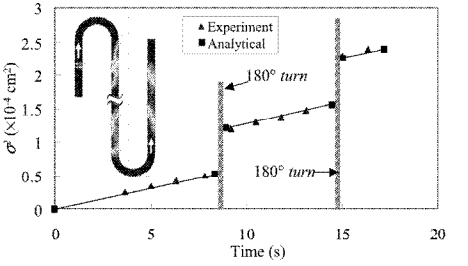

Fig. 4. Comparison of system simulation results with experimental data [3] (τ_t=0.048 and τ_{bt}=0.48).

In Figure 5, all parameters in Figure 4 are kept unchanged except for a reduced diffusivity, which leads to lower τ_t and τ_{bt}. The second turn now corrects the skew from

the first, leading to a reduced final variance. In Figure 6, the composable dispersion model for complex separation system involving up to six complimentary turns is compared to numerical simulation, in which τ_t ranges from 0.1 to 5×10^{-3} and τ_{bt} from 0.04 to 1.96×10^{-3}. A relative error of 9.5 % is found in the worst case when τ_t and τ_{bt} are very low. We observe that the variance increases with the number of complimentary turns in a linear, sublinear or superlinear relationship [6] depending on τ_t and τ_{bt}.

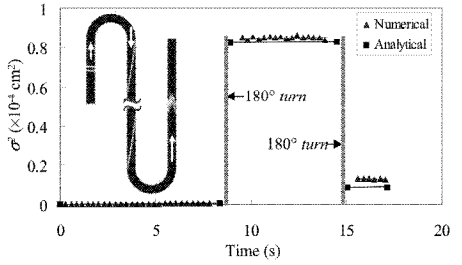

Fig. 5. Comparison of system simulation results with numerical data (τ_t=4.1×10^{-4} and τ_{bt}=4.1×10^{-3}).

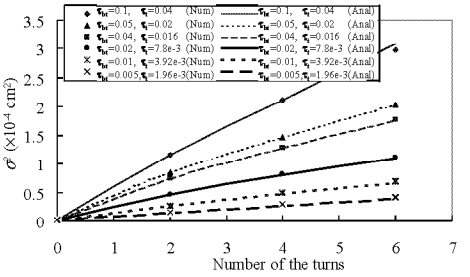

Fig. 6. Comparison of system simulation results of six complimentary turns with numerical data (w/R_C=0.2).

4. Conclusion

Analytical dispersion models have been presented for efficient simulations of complex microchip electrophoresis system. The models have been verified by numerical simulation and experimental data, and are able to accurately capture the combined effects of component geometry and analyte properties on analyte dispersion.

Acknowledgement

This research is sponsored by the DARPA and the Air Force Research Laboratory, Air Force Material Command, USAF, under grant number F30602-01-2-0587.

References

[1] S.K. Griffiths and R.H. Nilson, "Band Spreading in Two-Dimensional Microchannel Turns for Electrokinetic Species Transport," *Anal. Chem.*, Vol. 72, 5473-5482, 2000.

[2] J.I. Molho, A.E. Herr, B.P. Mosier, J.G. Santiago et.al, "Optimization of Turn Geometries for Microchip Electrophoresis," *Anal. Chem.*, Vol. 73, 1350-1360, 2001.

[3] C.T. Culbertson, S.C. Jacobson and J.M. Ramsey, "Dispersion Sources for Compact Geometries on Microchips," *Anal. Chem.*, Vol. 70, 3781-3789, 1998.

[4] Coventor, Inc., "Behavioral Models for Microfluidics Simulations," 2001.

[5] R. Aris., "On the Dispersion of a Solute in a Fluid Flowing through a Tube," Vol. 235A, *Proc. Roy. Soc. (London)*, 67-77. 1956.

[6] R.M. Magargle, J.F. Hoburg and T. Mukherjee, "A Simple Description of Turn-induced Transverse Field Dispersion in Microfluidic Channels for System-Level Design," *Proc. MSM*, San Francisco, CA., pp. 214-217, 2003.